Current Chemistry Letters 13 (2024) 425–434

Contents lists available at GrowingScience

Current Chemistry Letters

homepage: www.GrowingScience.com

Microwave-assisted synthesis and characterizations of nanosized copper ferrite and barium titanate for antimicrobial applications

Arunkumar Lagashetty[a*], K. Devendra[a], M. Sandhyarani[a], J. Rajeshwari[a], Galeppa[a], K.H. Lakshmidevi[a], B. B. Hajara[a], Veena V[b], Preeti R.K[c] and Sangappa K. Ganiger[d]

[a]*Department of Chemistry, Vijayanagara Sri Krishnadevaraya University, Ballari, 583105, Karnataka, India*
[b]*Department of Chemistry, Ballari Institute of Technology and Management, Ballari, 583105, Karnataka, India*
[c]*Department of Zoology, Gulbarga University, Kalaburagi, 585103, Karnataka, India*
[d]*Department of Physics, Government Engineering College, Huvinahadagali, 583219, Karnataka, India*

C H R O N I C L E

Article history:
Received March 20, 2023
Received in revised form
June 17, 2023
Accepted October 9, 2023
Available online
October 12, 2023

Keywords:
Bimetallic oxides
$BaTiO_3$
$CuFe_2O_4$
XRD
SEM
FT-IR
DX

A B S T R A C T

Science and technology of nanosized bimetallic oxide nanomaterials records the various properties and applications. Especially biomedical applications are viewed in particular due to its nanosized particle size. The present experimentation is reporting the microwave-assisted synthesis of nanosized bimetallic oxides like copper ferrite ($CuFe_2O_4$) and barium titanate ($BaTiO_3$) by solid state combustion route using poly (vinyl alcohol) (PVA) as a fuel. The structural and morphological characterizations of the bimetallic oxide nanomaterials are performed out by X-ray diffraction (XRD) and scanning electron micrograph (SEM) tools respectively. These analyses report the crystalline nature of both samples. EDX spectral study is also undertaken to know the existence of different metals in the above-mentioned samples. Bonding nature of the bimetallic oxide samples were readied by Fourier transfer infrared (FT-IR) instrumentation. The study reviewed the varied vibrational modes confirms the phase formation of the samples. UV-Vis and thermal study of these bimetallic oxide samples are also studied extensively to know the thermal and absorption behavior respectively. TGA of both the samples are traced and are showing decomposition at rapid rate. In addition, the maximum absorption peaks due to π - π^* transition confirms the sample formation. Antimicrobial activity of the prepared oxide samples was studied for antibacterial and antifungal behavior. Both samples showing considerable activity against various bacteria and fungi.

1. Introduction

Nanoscience is popularly defining by designing the functional materials at the nanoscale for its potential applications in various fields[1-3]. The reasons why nanoscale materials have become so important, because of its easy scale up synthesis, improved properties and need based applications [4-6]. Based on technology of nanomaterials is feathered to cover the design, utilization and construction of functional nanomaterials with at least one characteristic dimension[7-8]. Nanosized novel materials can be refigured to improve physical, chemical and biological properties in comparison with micro materials[9-11]. The reason behind such interesting development and useful behavior of these materials is due to structural features with intermediate in between isolated atoms and bulky materials. Hence, the objects may display physical substantially different from those displayed by either atoms or bulk materials lead to new technological opportunities as well as new challenges[12-14]. Bimetallic oxide nanomaterials are most important and are widely studied solid materials at nanoscale for various new properties for substantial applications[15-16]. Especially, nanosized transition metal oxides have attracted much due to their outer electron configuration and are applied widely in various reactions for their structural properties such as high surface area, variable pore size, and stability[17-19]. The current study materials like nanosized copper ferrite and barium ferrite materials falls under the same category and one can find superficial properties as well as applications in various fields.

* Corresponding author.
E-mail address arun.lagashetty@gmail.com (A. Lagashetty)

doi: 10.5267/j.ccl.2023.10.003

$CuFe_2O_4$ is a spinal type of oxide material which has high chemical stability, high thermal stability, high mechanical resistance and low surface acidity. In addition, this spinal material is suitable for various applications, such as high-density storage media, ferromagnetic fluids, catalysts, magnetic drug delivery systems, magnetic separation, magnetic resonance tomography, gas sensors, and another applications[20-23]. Copper based ferrite materials are having strong magnetic properties, relatively low conductivity, low eddy currents and dielectric losses. In continuation, it also shows the high permeability properties[24-25]. Similarly, barium titanate is one of the perovskite materials which can find various electronic and biological applications[26-27]. The ferroelectric and hydroelectric properties of barium ferrite are highly useful in manufacture of some varieties un-cooled sensors which are used in thermal cameras. Large crystals of barium ferrite are used in electronic precursors like capacitors, electrochemical transducers, and nonlinear optical tools.[28-29]. Recently, barium based titivate nanoparticles have been employed as nanocarriers for drug delivery in the body system[30-31]. It naturally occurring in barium-based perovskites and is very rare natural analogue of barium titanate found as micro inclusions in benitoite. In consideration of these including remarks, the present experimentation is reporting the synthesis of nanosized copper ferrite and barium titanate perovskite nanomaterials by self-propagating combustion route using PVA as a fuel. These bimetallic oxide nanomaterials were well characterized by various characterization tools for their phase formation. Antimicrobial activity studies of these prepared oxide materials are undertaken to know its antimicrobial behavior towards various bacteria and fungi.

2. Experimental

2.1 Materials and Methods

The chemicals used in the experimentation are of AR grade and are purchased from Merck (Mumbai, India) and are used with further purification. Properly rinsed glass wares with chromic acid are used in the experimentation for purity of the reaction product. Microwave-assisted self-propagating combustion route was adopted for the synthesis of barium titanate and copper ferrite nanomaterials using polymer as a fuel. For antimicrobial activity, nutrient agar (NA) and potato dextrose agar (PDA) media were purchased from Hi Media. The bacterial strains were of microbial type culture collection, procured from Institute of Microbial Technology, Chandigarh, India.

2.2 *Synthesis of the copper oxide and iron oxide nanomaterials*

Copper sulphate was thoroughly mixed with PVA in the weight ratio 1:5 and grounded well in a pestle and mortar. The resultant solid is transferred into China dish and was heated in an open air atmosphere until the completion of evolved carbonaceous fumes. The reaction undergoes self- propagating combustion reaction in presence of polymer fuel. Incomplete reaction product is transferred into a silica crucible and was ignited at around 800°C in muffle furnace. It was observed that, initially PVA melted, then frothed and finally ignited to give copper oxide as a residue[32]. Similar procedure was adopted for the synthesis of iron oxide nanomaterials by use of ferrous sulphate as a precursor material with same polymer fuel.

2.3 Synthesis of Copper ferrite and Barium titanate

Equimolar quantity of as prepared nanosized copper oxide and iron oxide was grinded well with PVA in the weight ratio of 1:1:5 in a pestle and mortar. The mixture was transferred into a crucible and was burnt initially on electric oven for complete evolution of fumes. Then, it is transferred to microwave oven for complete calcinations process. The sample was calcined on microwave oven having 2.45GHz frequency and power is 800w for about 15 minutes. During burning, the approximate temperature maintained around 1200°C.The reaction mixture burns suitably and leaving behind a solid copper ferrite as a crystalline product. Similar procedure is used for the synthesis of nanosized barium titanate nanomaterials sample. The obtained bimetallic oxide samples are shown in figure 1. Possible reactions involved in the combustion process are given below. The complete synthetic scheme of both the bimetallic oxides is given in **Scheme 1**.

$$CuO + Fe_2O_3 \rightarrow CuFe_2O_4$$
$$BaO + TiO_2 \rightarrow BaTiO_3$$

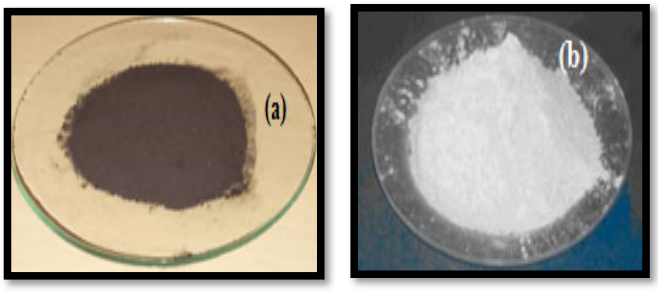

Fig. 1. Optical image of (a) $CuFe_2O_4$ nanomaterials (b) $BaTiO_3$ nanomaterials

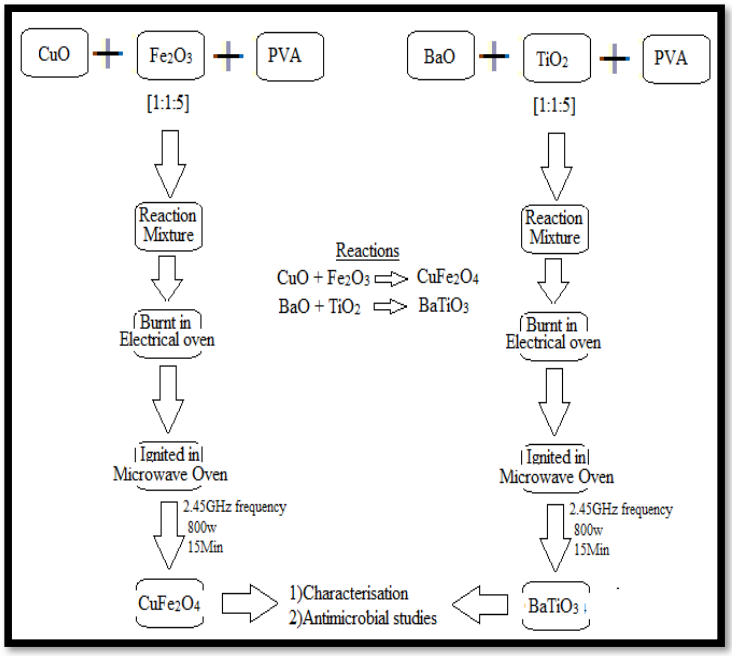

Scheme 1. Synthetic scheme of Copper ferrcopperd Barium titanate nanomaterials

2.3.1Antibacterial activity

Antibacterial activity of as prepared copper ferrite and barium titanate nanomaterial samples were performed by agar well diffusion method (Zhang *et al*., 2009) with minor modifications[33]. Petri dishes were prepared by inserting 20 ml sterilized NA media under regular condition and allowed to solidify. After media solidification, 100 µl of standard test microbial inoculums of gram-positive bacteria like *S. aureus*, *B. subtilis* and gram-negative bacteria like *S. Typhi*, and *Pseudomonas aeruginosa* were spread uniformly by use of sterile cotton swabs. 6 mm diameter agar is drawn from plate to form a well using sterile cork borer. Standard antibiotic gentamycin was considered and used as positive control, DMSO as negative control. After keeping at 4 ºC for 4 hours for the diffusion of antibacterial metabolites, thereafter plates were incubated at 37 ºC for 24 h. The antibacterial effect was estimated by taking a record of the growth inhibition zones in millimeters. The whole experiment was conducted in triplicate for proper confirmation of the activity.

2.3.2 Antifungal activity

Antifungal activity of prepared samples was studied by agar well diffusion method (Zhang *et al*., 2009) with required minor modifications[33]. Petri dishes were prepared by pouring 20 ml of PDA sterilized media under aseptic condition and allowed the same solidification. Soon after the solidification of the media, 100 µl of standardized test *Aspergilus niger* and *Fusarium* was spread uniformly using sterile L-shaped loop. 6 mm diameter agar is drawn from plate to form a wellbeing sterile cork borer for its spreading the sample. Antifungal Nystatin was used as positive control and DMSO as a negative control for the activity results. Samples kept at 4 ºC for 4 hours for the diffusion of antibacterial metabolites, thereafter these plates were incubated in reaction incubator at 28ºC for 72 h. The obtained diameter of the inhibition zone around the prepared well is measured in mm and the average of three best repeated agar discs were taken in to account to assess the strength of antifungal activity of the samples.

2.3.3 Characterization Techniques

The powder X-ray diffraction patterns of the samples were catalogued using JEOL JDX-8P diffractometer using CuKα radiation (1.54 Å) at 30 kV. The Fourier transform infrared (FTIR) spectra of the samples were recorded on a Perkin-Elmer FT-IR (Model No. 1000) in the range 4000-400 cm^{-1} at a resolution of 4 cm^{-1}. JEOL JSM-6380 LA scanning electron microscope with energy dispersive micro analysis of X-Ray (EDAX) is used to study particle morphology with metal confirmation of the sample. The absorption behavior of the sample was carried out by UV visible spectrophotometric measurements using Elico spectrophotometer. Technai-20 Philips transmission electron microscope operated at 190 KeV to carry out TEM images. Metllor Toledo star tool was used to trace the thermal characterization.

3. Results and discussion

3.1 FT-IR study

Fig. 2(a-b) shows FT-IR spectra of combustion derived copper ferrite and barium titanate samples respectively. The metal- oxygen bonding and nature of the synthesized bimetallic oxide samples were carried out by infrared study. Generally

metal oxides give absorption bands below 1000cm^{-1} arising from inter-atomic vibrations[34]. It is observed in both spectra that, the peak at 3500cm^{-1} corresponds to absorption of moisture content. Further, the vibration band observed at 1050 cm^{-1}is due to some overtones. Peaks below 1000 cm^{-1} corresponds to Metal-oxygen vibrational modes and metal-metal vibration modes of the readied sample confirm the phase formation of prepared bimetallic oxide samples[35].

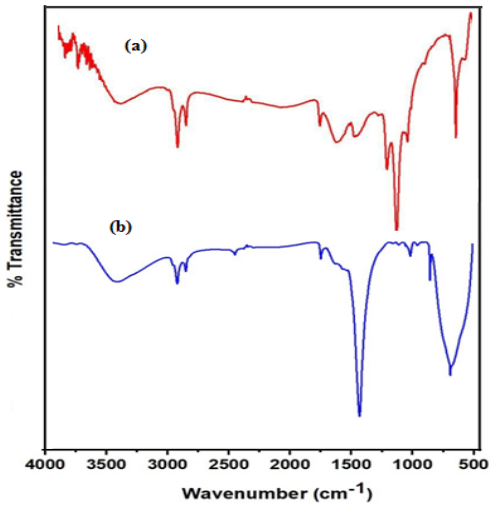

Fig. 2. FT-IR of (a) $CuFe_2O_4$ nanomaterials (b) $BaTiO_3$ nanomaterials

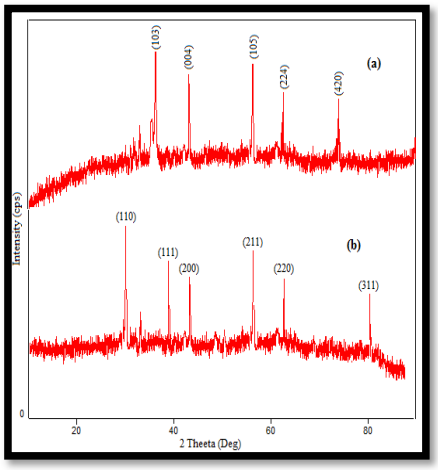

Fig. 3. Indexed XRD pattern (a) $CuFe_2O_4$ nanomaterials (b) $BaTiO_3$ nanomaterials

3.2 XRD Study

XRD system was used to know the crysallinity and phase structure of the as-synthesised bimetallic oxide samples. **Fig. 3(a-b)** represents the indexed XRD pattern of as synthesized copper ferrite and barium titanate nanomaterials respectively. According to the XRD pattern, obtained 2ɵ values and (hkl) values of both samples are indexed in accordance with standard JCPDS values and are tabulated in table-1. Both patterns show the presence of highly intense Bragg's reflections indicates the crystalline nature of both samples. It is also illustrating that, at higher temperature samples showing stable structure. The intensity of peaks in the pattern are sharp indicates the high crystalline nature of both the samples. These patterns not demonstrating monometallic oxide reflections which are utilized for bimetallic oxide sample preparation. It is observed from the table and indexed pattern, the most of the 2ɵ (or d-spacing) value of the sample acceptably matches with literature data of the copper ferrite (JCPDS card No. 34-0425) and barium titanate (JCPDS card No.79-2264) confirms the formation of $CuFe_2O_4$ and $BaTiO_3$ nanomaterials respectively with single crystalline phase. Further, the existence of the indexed major lattice planes in the pattern supports the sample formation. The broadening and sharp peaks indicate the reduced particle size and high crystallinity of the samples. It is also noticed that, at the higher temperature the removal of extra undefined phases. Purity of the samples analyzed in the pattern by the absence of the other reflection[36].

Table 1. XRD data of $BaTiO_3$ and $CuFe_2O_4$ samples

Sl.No	$CuFe_2O_4$		$BaTiO_3$	
	Observed 2ɵ values	(hkl)	Observed 2ɵ values	(hkl)
1	35.02	(103)	32.33	(110)
2	43.10	(004)	39.43	(111)
3	56.11	(105)	46.82	(200)
4	62.00	(224)	57.64	(211)
5	73.33	(420)	67.50	(220)
6	-----	---	80.05	(311)

3.3 EDX Study

The EDX analyses of the bimetallic oxide samples were performed to clarify its elemental compositions. **Fig. 4 (a-b)** shows the EDX pattern of combustion derived $CuFe_2O_4$ and $BaTiO_3$ nanomaterials respectively. The chemical constituents like presence of Cu, Fe, and O elemental segments are observed at respective position in the EDX pattern of copper ferrite (**Fig. 4(a)**) confirms the formation of the said sample. Similarly, the reflections of Ba, Ti and O elemental segments in the EDX pattern of barium titanate (**Fig. 4(b)**) signify the formation of sample. No other elemental reflections other than the above observed indicates the purity of the prepared samples.

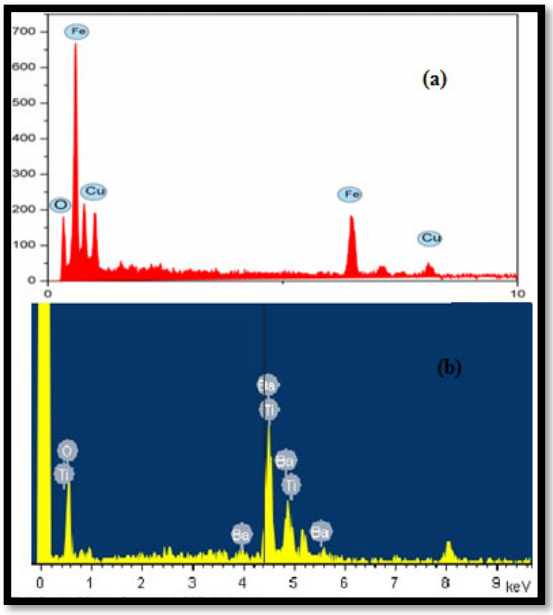

Fig. 4. EDX pattern of (a) $CuFe_2O_4$ (b) $BaTiO_3$ nanomaterials

3.4 SEM study

The surface morphology of the prepared nanomaterial was examined through SEM instrumentation. Figure 5(a-b) shows SEM images of $CuFe_2O_4$ and $BaTiO_3$ nanomaterials respectively. Several cracks are observed due to the existence of the voids, which originates from the pore boundaries and then propagate to maximum compression direction. The grain morphology, uniformity, homogeneity, and their distribution have been observed. Copper ferrite particles showed large grains stuck to each other in an irregular and non-uniform manner is observed in **Fig. 5(a)**. The SEM image of barium titanate (**Fig. 5(b)**) shows that the particles fall in the nano-orange with fine, spherical shaped particles with regular arrangement. Some particles show clear close compactness of the particles indicated the very crystalline nature and also lead to applicable morphology. It is also noticeable that the particle sizes differed from the crystalline sizes due to polycrystalline agglomeration with a single crystal. These results are in close consideration with XRD results in terms of its crystalline behavior.

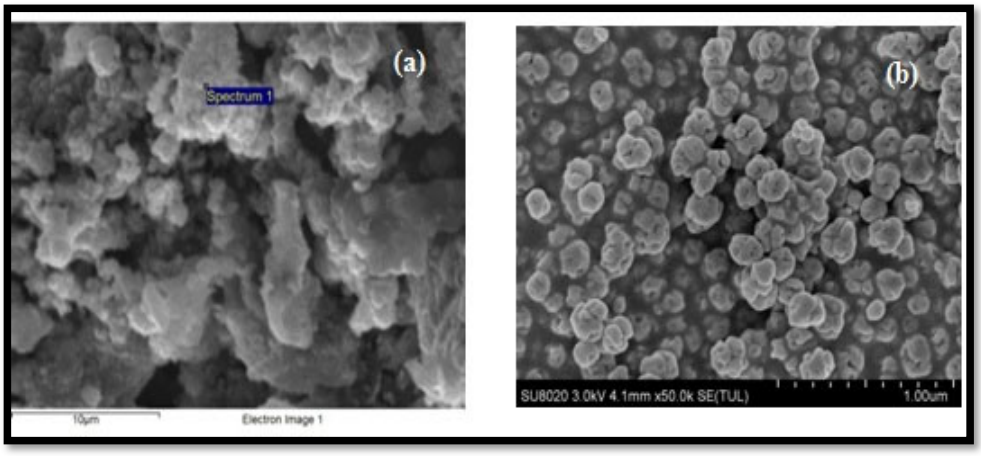

Fig. 5. SEM image of (a) $CuFe_2O_4$ (b) $BaTiO_3$ nanomaterials

3.4 TEM Study

Particle morphology and its size of the combustion derived $CuFe_2O_4$ and $BaTiO_3$ nanomaterials samples was studied by TEM instrumentation and its images are represented in **Fig. 6(a-b),** respectively. **Fig. 6(a)** shows the crystalline nature of the sample and is in accordance with XRD results. It is also highlighting particle netting falls under nano size range diameters. However, the image further reveals that some particles are spherical, and some are irregular particles nature in agreement with SEM results.

Similarly, barium titanate nanomaterials also show crystalline behavior and its SEM image is given in figure 6(b). In addition, particle agglomeration with particle compactness is also viewed in the said image.

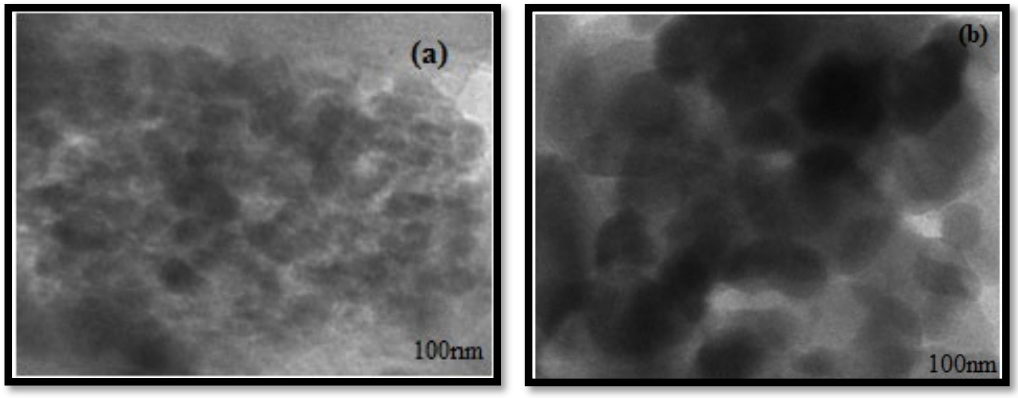

Fig. 6. TEM image of (a) $CuFe_2O_4$ (b) $BaTiO_3$ nanomaterials

3.5 Thermal Study

TGA study is carried out to view the sequential weight loss and subsequent transformation due to heat treatment of the samples. **Fig. 7(a-b)** shows the TGA traces of $CuFe_2O_4$ and $BaTiO_3$ samples respectively. It is observed from **Fig. 7(a)** that the three-step decomposition under exited temperature range 100-500ºC, 500-650ºC and 650-1000ºC. Copper ferrite sample shows the initial weight loss in the range 100-500ºC is due to water evaporation. Further, the sample decomposes continuously as the temperature rises and shows a sharp weight loss in the range 500ºC-650ºC due to further decomposition of residual precursor oxides present in the sample. Above 900ºC, no weight loss was observed indicates the decomposition of the phases of the sample. Similar features are observed in barium titanate sample. TGA trace of barium titanate sample (**Fig. 7(b)**) is also showing significant three step weight loss in the temperature range 100-400ºC, 400-500ºC and 500-800ºC. The initial weight loss is due to evaporation of water and second loss is due to further residual oxides decomposition and third loss is due to decomposition of complete phase of the sample.[37-38]

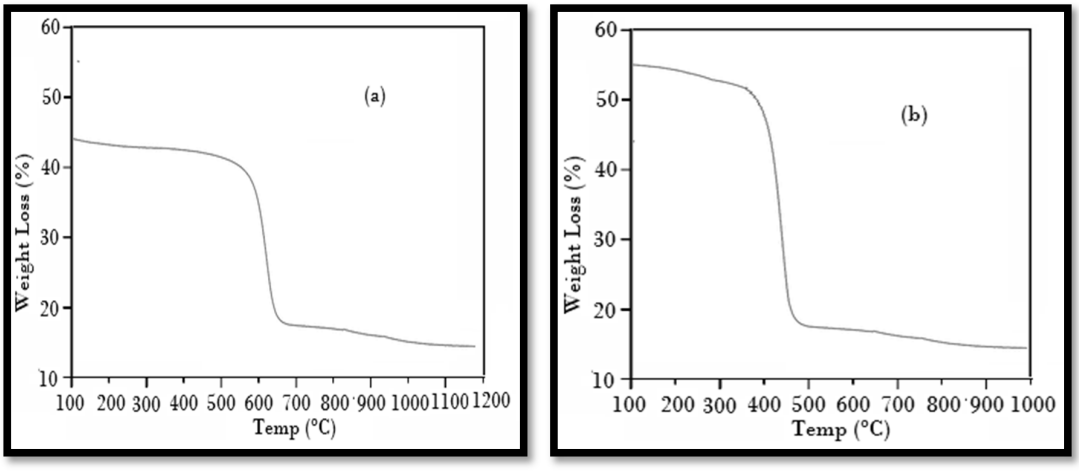

Fig. 7. TGA trace of (a) $CuFe_2O_4$ (b) $BaTiO_3$ nanomaterials

3.6 UV-Vis study

Optical properties of bimetallic samples were well studied by UV-Vis spectroscopic analysis. The absorption spectra of $CuFe_2O_4$ and $BaTiO_3$ samples are shown in **Fig. 8(a-b)**, respectively. It is observed from UV-Vis absorption spectra of $CuFe_2O_4$ that, a single and maximum strong surface Plasmon resonance band (λ_{max}) at 350nm is assigned to the characteristics phase of $CuFe_2O_4$. Similarly, a single maximum strong surface Plasmon resonance band (λ_{max}) at 310nm (in **Fig. 8(b)**) is observed due to excitation of electron from valence band to conduction band and the characteristics phase of $BaTiO_3$ sample. Both samples show the broad Plasmon bands with an absorption tail in the higher wavelength.

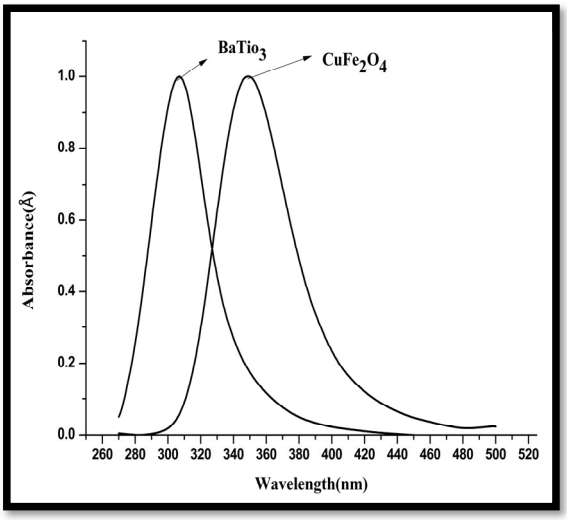

Fig. 8. UV-Vis spectra of $CuFe_2O_4$ and $BaTiO_3$ nanomaterials

3.7 Antibacterial activity

Observed antibacterial results of the prepared $BaTiO_3$ and $CuFe_2O_4$ samples are given in **Table 2** and results are represented graphically in **Fig. 9**. It is observed from the table that; the samples show good activity at higher concentration in comparison with standard drug.

Table 2. Antibacterial results of $BaTiO_3$ and $CuFe_2O_4$ samples

Sl.No	Name of the samples	Conc. (µg/ml)	*S. aureus* (mm)	*B. subtilis (mm)*	*S. Typhi* (mm)	*Pseudomonas A (mm)*
1	$BaTiO_3$	25	0	0	0	0
	$CuFe_2O_4$		0	0	0	0
2	$BaTiO_3$	50	3	4	4	4
	$CuFe_2O_4$		4	6	5	5
3	$BaTiO_3$	75	9	10	9	10
	$CuFe_2O_4$		10	10	10	11
4	$BaTiO_3$	100	12	12	12	13
	$CuFe_2O_4$		12	13	12	12
5	$BaTiO_3$	200	12	13	13	13
	$CuFe_2O_4$		14	14	14	14
6	Gentamycin (Standard)	100	15mm	15	15	15

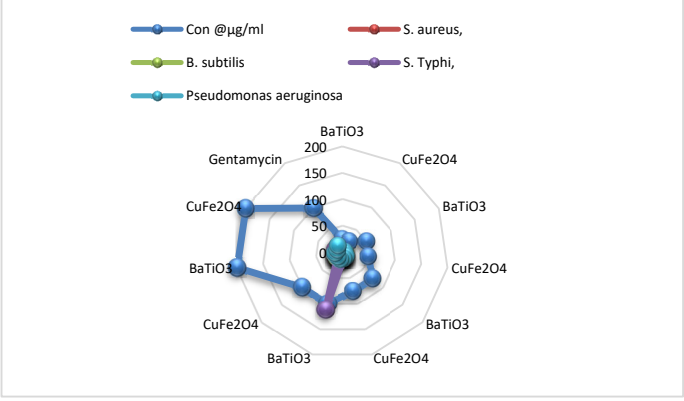

Fig. 9. Graphical representation of antibacterial activity of $CuFe_2O_4$ $BaTiO_3$ nanomaterials

In addition, both the samples show the same activity range for all bacteria at the same concentration. The increasing use of nanoparticles (NPs) in medicine has led to an enhanced number of studies declaring the potential antibacterial mechanisms of NPs against bacteria. The nanosized sample materials are made in contact with bacterial cells to achieve their antibacterial functional performance. The acceptable forms of contact include electrostatic attraction[39] van der Waals forces[40], receptor–ligand[41] and hydrophobic interactions[42]. From the mentioned figure, it is also observed that antimicrobial activity was performed to understanding the molecular biology mechanism associated with the bactericidal action of $BaTiO_3$ and $CuFe_2O_4$ nanomaterials. In comparison, $CuFe_2O_4$ nanomaterials exhibited good antibacterial results compared to nanosized $BaTiO_3$ sample. The reason is that the combination of copper and iron oxide nanomaterials can adhere to the

surface of bacterial cells to produce ROS and damage the composition as well as structure of the cell membrane[43]. There by interfering with the function of the cell membrane and causing leakage of cellular contents, resulting in bacterial death.

3.8 Antifungal activity

The growths of the tested fungal species were significantly inhibited by the synthesized nanoparticles. From the obtained results it is confirming that the MIC of the tested fungal species was at 100 µg mL^{-1}.The observed antifungal activity results are given in table-3 and results are represented graphically in figure 10. The table clearly indicated that the $CuFe_2O_4$ nanomaterials exhibited good antifungal activity compared to $BaTiO_3$ nanomaterials. Both the samples show good antifungal activity at higher concentration in comparison with standard drug. Further, both fungi show the same activity range for respective concentration. $CuFe_2O_4$ nanomaterials would allow a higher level of penetration of free radicals or ions causing cell death at lower concentrations [44]. Nanomaterials with the smaller size can interact quickly with the cell wall and membrane causing leakage of genetic materials, proteins, and minerals that finally result in cell death [45].

Table 3. Antifungal activity results of $BaTiO_3$ and $CuFe_2O_4$ samples

Sl. No.	Sample	Conc. (µg/ml)	*Anti-fungal Aspergilus niger(mm)*	*Fusarium. S (mm)*
1	$BaTiO_3$	25	4	5
	$CuFe_2O_4$		4	5
2	$BaTiO_3$	50	6	6
	$CuFe_2O_4$		6	6
3	$BaTiO_3$	75	7	9
	$CuFe_2O_4$		8	11
4	$BaTiO_3$	100	9	10
	$CuFe_2O_4$		9	12
5	$BaTiO_3$	200	11	10
	$CuFe_2O_4$		10	11
6	Nystatin (standard)	100	12	12

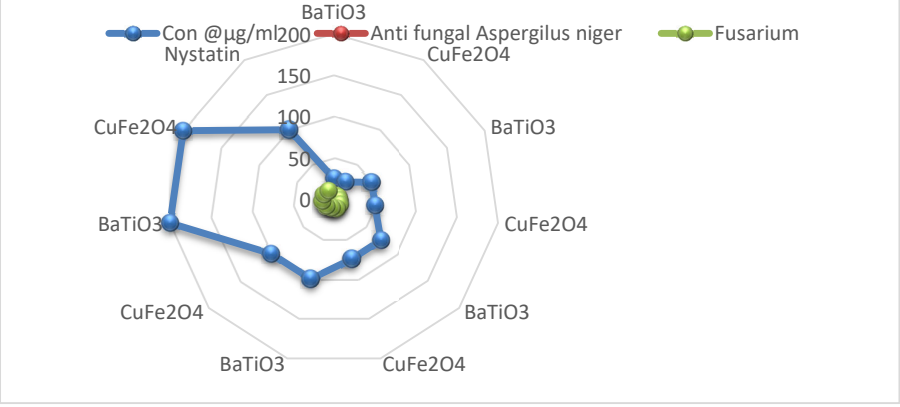

Fig. 10. Graphical representation of antifungal activity of $CuFe_2O_4$ and $BaTiO_3$ nanomaterials

4. Conclusions

The successful synthesis of nanosized copper ferrite and barium titanate is achieved by combustion route with PVA as a fuel. This self-propagating solid state combustion reaction achieved the phase formation of bimetallic oxide samples with simple experimentation. This method may be one of the prominent routes for the synthesis of other bimetallic oxide nanomaterials like perovskites. The synthesized nanoparticles showed potent antibacterial and antifungal activities against the tested pathogens. Consequently, the synthesized $CuFe_2O_4$ nanoparticles showed better activity compared to $BaTiO_3$ nanomaterials. Results of the current study reflect that $CuFe_2O_4$can be better explored soon for various biomedical, industrial, and agricultural applications. Moreover, the high yield of the copper ferrite nanoparticles achieved in the present study could open up the way for the manufacture of nanoparticles at an industrial scale using a cost-effective and eco-friendly methodology.

Acknowledgement

Authors thank DST-FIST (SR/FST/CSI-003/2016) grant provided for instruments and infrastructure facilities to VSK University, Ballari. Thanks are due to Prof. A.Venkataraman, Professor, Department of Chemistry, Gulbarga University, Kalaburagi, Karnataka, India for useful discussion in spectral analysis.

References

1. Ngonidzashe Masunga., Olga Kelebogile Mmelesi., Kebede K. Kefeni., Bhekie B. Mamba. **(2019)** Recent advances in copper ferrite nanoparticles and nanocomposites synthesis, magnetic properties and application in water treatment: Review, *J. Env.Chem.Engg.7(3),* 103179.
2. Faten Haithum Mulud., Najat A., Dahham., Ibrahim F., Waheed. **(2020)** Synthesis and characterization of copper ferrite nanoparticles, *IOP Conf. Ser. Mater. Sci. E*ng. 928, 072125.
3. Pragnesh Dave N., Thakkar R., Ruksana Sirach., Shalini Chaturvedi. **(2022)** Effect of copper ferrite ($CuFe_2O_4$) in the thermal decomposition of modified nitrotriazolone, *Mater. Adv.,* 3, 5019 – 5026.
4. Tarun Kumar Barik., Gopal Chandra Maity., Pallavi Gupta., Mohan L., Tuhin Subhra Santra. **(2021)** Nanomaterials: An Introduction, *Nanomaterials and their Biomedical Applications,* 1, 27.
5. Velinov N., Petrova T., Ivanovna., Tsoncheva T., Kovacheva D., Mitov I. **(2021)** Synthesis Mossbauer study and catalytic properties of Cu-Ni-Fe- oxide/nitride mixed-phase materials, *Hyperfine Interact*, 242, 1-12.
6. Wang W., Guo S., Zhang D., Yang Z. **(2019)** One-pot hydrothermal synthesis of reduced graphene oxide/zinc ferrite nano hybrids and its catalytic activity on the thermal decomposition of ammonium perchlorate*, Journal Saudi Chem. Soc.*, 23, 133-140.
7. Pham T. N., Huy T. Q. **(2020)** Spinel ferrite (AFe_2O_4)-based hetero-structured designs for lithium-ion battery environmental monitoring and biomedical applications*, RSC,* 10, 31622-31631.
8. Chen Q. W. D., Wang R., Shen G. **(2015)** Ternary oxide nanostructured materials for supercapacitors a review, *J. Mater. Chem. A*, 3, 10158 – 10173.
9. Yang Z., Zhang Z., Jiang Y., Chi M., Nie G., Lu X., Wang C. **(2016)** Palladium nanoparticles modified electro spun $CoFe_2O_4$ nanotubes with enhanced peroxidase-like activity for colorimetric detection of hydrogen peroxide, *RSC Adv,* 6, 33636 -33642.
10. Abu-Hani A. F. S., Mahmoud S. T., Awwad F., Ayesh A. I. **(2017)** Design fabrication and characterization of portable gas sensors based on spinel ferrite nanoparticles embedded in organic membranes, *Sens. and Actuators, B*, 214, 1179 – 1187.
11. Peeples B., Goornavar V., Peeples C., Spence D., Parker V., Bell C., Biswal D., Ramesh G. T., Pradhan A. K. **(2014)** Structural, stability, magnetic, and toxicity studies of nanocrystalline iron oxide and cobalt ferrites for biomedical applications, *J. Nano part. Res.,* 16, 2290.
12. Kim H., Lee J. W., Byun D., Choi W. **(2018)** Coaxial-nanostructured $MnFe_2O_4$ nanoparticles on polydopamine-coated MWCNT for anode materials in rechargeable batteries, *Nanoscale,* 10, 18949 – 18960.
13. Galvao W. S., Neto D. M. A., Freire R. M., Fechine P. B. A. **(2015)** Super-Paramagnetic nanoparticles with spinel structure: A Review of synthesis and biomedical applications, *Solid State Phenom,* 241, 139 – 176.
14. Kumar M., Singh Dosanjh H., Sonika Singh J., Monir K., Singh H. **(2020)** Review on magnetic nano ferrites and their composites as alternatives in waste water treatment: synthesis, modifications and applications, *Environ. Sci. Water Res. Technol,* 6, 491 – 514.
15. Elango Balaji T., Himadri Tanaya Das., Maiyalagan T. **(2021)** Recent trends in bimetallic oxides and their composites as electrode materials for super-capacitor applications, *Electro Chem. 8(10*), 1723 – 1717.
16. Diaz C., Valenzuela M. L., Laguna-Bercero M. A. **(2022)** Solid-state preparation of metal and metal oxides nanostructures and their application in environmental remediation, *Int. J. Mol. Sci.* 23, 1093.
17. Diaz C., Valenzuela M. L., Garcia C., Campa De la R., Soto A. P. **(2017)** Solid-state synthesis of pure and doped lanthanides oxide nanomaterials by using polymer templates. Study of their luminescent properties. *Mater. Lett*. 209, 111 – 114.
18. Ray C., Pai T. **(2017)** Recent advances of metal–metal oxide nanocomposites and their tailored nanostructures in numerous catalytic applications, *J. Mater. Chem*, 5, 9465 – 9478.
19. Yattinahalli S. S., Kapatkar S. B., Ayachith N. H. **(2013**) Synthesis and structural characterisation of nanosized nickel ferrite, *International Journal of Self Propagating High Temperature Synthesis,* 22, 147-150.
20. Maleki A., Hajizadeh Z., Salehi P. (**2019**) Mesoporous halloysite nanotubes modified by $CuFe_2O_4$ spinel ferrite nanoparticles and study of its application as a novel and efficient heterogeneous catalyst in the synthesis of pyrazolopyridine derivatives, *Sci. Rep.* 9, 5552.
21. Mirzaei M., Habibi M. H., Sabzyan H. **(2022)** Synthesis characterization and dye degradation photocatalytic activity of the nano-size copper iron binary oxide, *Environ Sci. Pollut, Res,* 29, 9173 – 9192.
22. Kamel A. H., Hassan A. A., Amr A. E., El-Shalakany H. H., Al-Omar M. A. **(2020)** Synthesis and characterization of $CuFe_2O_4$ nanoparticles modified with Polythiophene: applications to mercuric ions removal, *Nanomaterials,* 10, 586 – 598.
23. Younes A., Kherrouba N., Bouamer A. **(2021)** Magnetic optical structural and thermal properties of copper ferrite nanostructured synthesized by mechanical alloying, *Micro Nano Lett,* 16, 251 - 256; DOI; https://doi.org/10.1049/mna2.12040.
24. Qin Q., Liu Y., Li X., Suna T., Xu Y. **(2018)** Enhanced heterogeneous Fenton-like degradation of methylene blue by reduced $CuFe_2O_4$, *RSC Adv,* 8, 1071.

25. Anandan S., Selvamani T., Asiri A. M., Wu J. J. **(2017)** Magnetic and catalytic properties of inverse spinel $CuFe_2O_4$ nanoparticles, *J. Mag. J. Mater,* 15, 437- 443.
26. Ahamed M., Akhtar M. J., Khan M. A. M., Alhadlaq H. A., Alshamsan A. **(2020)** Barium Titanate ($BaTiO_3$) nanoparticles exert cytotoxicity through oxidative stress in human lung carcinoma (A549) cells. *Nanomaterial's (Basel).* 10(11), 2309.
27. Genchi G., Attilio Marino., Antonella Rocca., Mattoli V., Ciofani G**. (2016)** Barium titanate nanoparticles: promising multitasking vectors in nanomedicine, *Nanotechnology*, 27(23), 27 – 35.
28. Wen-Bo Li., Di Zhou., Ran Xu., Da-Wei Wang., Jin-Zhan Su., Li-Xia Pang., Wen-Feng Liuand., Guo-Hua Chen. **(2019)** $BaTiO_3$-Based multilayers with outstanding energy storage performance for high temperature capacitor applications, *ACS Appl. Energy Mater,* 2**(**8**)**, 5- 5506.
29. Huijing Yang., Weichao Bao., Zhilun Lu., Linhao Li., Hongfen Ji., Yuhe Huang., Fang fang Xu., Ge Wang., Dawei Wang. (**2021)** High-energy storage performance in $BaTiO_3$-based lead-free multilayer ceramic capacitors, *Journal of Materials Research, 36*(6), 1285-1294.
30. Fakhar-e-Alam M., Samira Saddique., Nazia Hossain., Aamir Shahzad., Inaam Ullah., Amjad Sohail., Muhammad Junaid Iqbal Khan., Malik Saadullah. **(2023)** Synthesis characterization, and application of $BaTiO_3$ nanoparticles for anti-cancer activity, *Journal of Cluster Science*, 34, 1745-1755.
31. Jordan T., Mikaela O Brien A., Catalina-Paula., Spatarelu., Geoffrey P., Luke. **(2020)** Antibody-conjugated barium titanate nanoparticles for cell-specific targeting. *ACS Appl. Nano Mater.* 3, 2636 – 2646.
32. Arunkumar Lagashetty., Amrutha Pattar., Sangappa K Ganiger. **(2019)** Synthesis characterization and antibacterial study of Ag doped magnesium ferrite nanocompoiste, *Heliyon* 5, e01760.
33. Zuhair S., Abeer A., Kassem Ragwa., Mohamed Farad., Shaimaa Khamis Mostafa., Gihan Salah Labib. **(2022)** Nano-carrier drug delivery systems: characterization, limitations, future perspectives and implementation of artificial intelligence, *Pharmaceutics.*18, 14(4), 883.
34. Arunkumar Lagashetty., Sangappa K. Ganiger., Preeti R. K., Shashidhar Reddy., Malathesh Pari. **(2020)** Microwave-assisted green synthesis, characterization and adsorption study of metal oxide nanoparticles by *Ficus Benghalensis* plant leaf extract, *New Journal of Chemistry* 14(33), 14095 – 14102.
35. Mounesh T. M., Sharankumar N.Y., Praveen Kumar K. R., Venugopala Reddy K. B., Chandrakala., Arunkumar L., Vidyasagar C. C. **(2021)** Novel Schiff base cobalt (II) Phthalocyanine with appliance of MWCNTs: Enhanced electro-catalytic activity behaviour of α-amino acids, *RSC Advances.* 11, 16736-16746.
36. Arunkumar Lagashetty., Vibhav Mittin., Manjunath K. Patil., Sangappa K. Ganiger. **(2020)** Synthesis, Characterization and Studies of $BaFe_2O_4$/PMMA nanocomposites, *Polymer Bulletin*, 78(10), 5905 – 5921.
37. Synkiewicz-Musialska B., Kulawik J., Czerwińska E., Pałka N. **(2023)** Novel copper borate ceramics with lithium-based sintering aids for LTCC terahertz applications, *J. Mater. Chem. C,* 11, 1863 – 1871.
38. Szwagierczak D., Synkiewicz-Musialska B., Kulawik., Czerwińska E., Pałka N., Bajurko P. **(2020)** Low temperature sintering of $Zn_4B_6O_{13}$ based substrates, their microstructure and dielectric properties up to the THz range, *Journal of Alloys and Compounds,* 819(5), 153025.
39. Chen Li H., Zhao Q. J., Urmila K. **(2015)** Enhancing the antimicrobial activity of natural extraction using the synthetic ultra-small metal nanoparticles. *Sci Rep.* 5, 11033.
40. Ilaria Armentano., Carla Renata Arciola., Elena Fortunati., Davide Ferrari., Samantha Mattioli., Concetta Floriana Amoroso., Jessica Rizzo., Jose M Kenny., Marcello Imbriani., Livia Visai. **(2014)** The interaction of bacteria with engineered nanostructured polymeric materials: a review. *Scientific World J.* 5, 410423.
41. Gao W., Thamphiwatana S., Angsantikul P., Zhang L. **(2014)** Nanoparticle approaches against bacterial infections. *Wires Nanomed Nanobi*. 6(6), 532 – 547.
42. Luan B., Huynh T., Zhou R. **(2016)** Complete wetting of graphene by biological lipids, *Nanoscale,* 8(10), 5750 - 5754; DOI; https://doi.org/10.1039/C6NR00202A
43. Foster H. A., Ditta, I. B., Varghese S., Steele A. **(2011)** Photocatalytic disinfection using titanium dioxide: spectrum and mechanism of antimicrobial activity. *Appl Microbiol Biotechnol*. 90(6), 1847 – 1868.
44. Ismail R. A., Suliman G.M., Abdurrahman S. A., Marzoog T. R. **(2015)** Antibacterial activity of magnetic iron oxide nanoparticles synthesized by laser ablation in liquid, *Mater. Sci. Eng. C,* 53, 286 – 297.
45. Hamilton D., Jones S. K., Orr Mallapragada., Narasimhan B., Canfield P. C., Prozorov R. **(2007)** Cobalt ferrite nano crystals: out-performing magneto tactic bacteria, *ACS Nano,* 1, 228 – 233.